Theme: National and International Governance Challenges.

Cellular automata and Genetic Algorithms based urban growth visualization for appropriate land use policies

Uttam Kumar[1] [uttam@ces.iisc.ernet.in]
Mukhopadhyay C.[2] [cm@mgmt.iisc.ernet.in]
&
Ramachandra T. V.[3],* [cestvr@ces.iisc.ernet.in]

[1] Department of Management Studies & Centre for Sustainable Technologies, Indian Institute of Science, Bangalore.
[2] Department of Management Studies, Indian Institute of Science, Bangalore.
[3] Centre for Ecological Sciences; Centre for Sustainable Technologies & Centre for Infrastructure, Sustainable Transport and Urban Planning (C*i*STUP), Indian Institute of Science, Bangalore.

Citation: Uttam Kumar, Chiranjit Mukhopadhyay and Ramachandra T. V., (2009), Cellular automata and Genetic Algorithms based urban growth visualization for appropriate land use policies, Proceedings of the Fourth Annual International Conference on Public Policy and Management, Centre for Public Policy, Indian Institute of Management (IIMB), Bangalore, India, 9-12 August, 2009.

Cellular automata and Genetic Algorithms based urban growth visualization for appropriate land use policies

Abstract

Many regional environmental problems are the consequence of anthropogenic activities involving land cover changes. Temporal land cover data with social aspects are critical in tracing relationships of cause and effect on variables of interest with the effects of context on behaviour or with the process of human environment interaction and are also useful for governance of urbanising cities. Many cities are now undergoing redevelopment for economic purposes with new roads, infrastructure improvements, etc. This phenomenona is very rapid in India with urban population growing at around 2.3 percent per annum. This dramatic increase in urbanisation has raised the necessity to understand the dynamics of urban growth process for planning of natural resources. Cellular automata, an artificial intelligence technique based on pixels, states, neighbourhood and transition rules, is being implemented to model the urban growth process due to its ability to fit such complex spatial nature using simple and effective rules. The possibility of using genetic algorithms for automatic calibration of the model through proper design of their parameters, including objective function, initial population, selection, crossover and mutation has also been explored. The techniques are tested for Bangalore city, India by modeling the urban growth using remote sensing data of various resolutions.

Key words: land use model, urban growth, cellular automata, governance

1. Introduction

Urban growth modeling is getting more attention as an emerging research area in many disciplines. Urbanisation is a form of metropolitan growth that is a response to often bewildering sets of economic, social, and political forces and to the physical geography of an area. This comes as a result of the recent dramatic increase in urban population that increases the pressure on the infrastructure services. Many cities are now undergoing redevelopment for economic purposes with new roads, infrastructure improvements, etc. This phenomenona is very rapid in India with urban population growing at around 2.3 percent per annum (World Urbanization Prospects, 2005). An increased urban population and growth in urban areas is irreversible with population growth and migration. This dramatic increase in urbanisation has raised the necessity to understand the dynamics of urban growth process for planning of natural resources. It also raises the necessity to understand the dynamics of urban growth process through "growth models" for sustainable distribution of usable resources.

Among the developed growth models, cellular automata (CA), an artificial intelligence technique based urban growth models have better performance in simulating urban development than conventional mathematical models (Batty and Xie, 1994). CA simplifies the simulation of complex systems (Waldrop, 1992). Its aptness in urban modelling is due to the fact that the process of urban spread is entirely local in nature (Clarke and Gaydos, 1998). CA is based on pixels, states, neighbourhood and transition rules, and is being implemented to model the urban growth process due to its ability to fit complex spatial nature using simple and effective rules. Development of CA model involves rule definition and calibration to produce results consistent with historical data, and future prediction with the same rules (Clarke et al., 1997). Many CA-based urban growth models are reported in literatures including the model by White and Engelen (1992; 1993) that involves reduction of space into square grids. They implement the defined transition rules in recursive form to match the spatial pattern. One of the earliest and most well-known models is CA-based "SLEUTH" model that has four major types of data: land cover, slope, transportation, and protected lands (Clarke's et al., 1997). This is rooted in the work of von Neumann (1966), Hagerstrand (1967), Tobler (1979) and Wolfram (1994). A set of initial conditions in SLEUTH is defined by 'seed' cells which are determined by locating and dating the extent of various settlements identified from historical maps, atlases, and other sources. These seed cells represent the initial distribution of urban areas. A set of complex behaviour rules are developed that involves selecting a location randomly, investigating the spatial properties of the neighboring cells, and urbanising the cell based on a set of probabilities.

Despite these achievements in CA urban growth modeling, the selection of CA transition rules remains a research topic. Most of the CA models are usually designed based on individual preference and application requirements with transition rules being defined in an ad hoc manner (Li and Yeh, 2003). Furthermore, most of the developed CA models need intensive computation to select the best parameter values for accurate modeling. This motivates development and implementation of an effective CA-based urban growth model that is easy to calibrate and takes into account the *spatial* and *temporal* dynamics of urban growth simultaneously. The objectives of this study are:

(i) To develop and implement an effective CA-based urban growth model to simulate the growth as a function of local neighbourhood structure of the input data.

(ii) To develop a calibration algorithm that takes into consideration spatial and temporal dynamics of urban growth.

Spatially, the model is calibrated locally to take into account the effect of site specific features while the temporal calibration is set up to adapt the model to the changes over growth pattern with time. Calibration provides the optimal values for the transition rules to achieve accurate urban growth modeling. The input to the urban growth model consists of two types of data:

(i) classified images of 1973, 1992 and 2006 where each pixel represents one of the four land use classes – urban, vegetation, water and others.

(ii) population density maps being represented by pixels in a raster format for the year 1973 and 1992.

CA generates transition rules for each pixel based on the current state of the pixel's category (in terms of land use class) and population density value of that pixel together, to decide the next state of the pixel after a time epoch, i.e. change in land use from one class to another from 1973 to 1992 and 1992 to 2006. The model is tested for Bangalore city, India by modeling the growth using remote sensing data of various spatial, spectral and temporal resolutions. Later, towards the end of this communication, genetic algorithm (GA) is introduced as a heuristic optimisation technique for selecting optimal model parameters. The possibility of using GA for automatic calibration of the model through proper design of their parameters, including objective function, initial population, selection, crossover and mutation has been explored. Here, a set of strings are used as initial population over which GA runs till convergence.

The paper is organized as follows: section 2 briefs the study area, followed by data preparation details in section 3 – classification of remote sensing data of three time periods (1973, 1992 and 2006) and generation of population density maps corresponding to the year 1973 and 1992. Section 4 introduces CA; section 5 presents the simulated results from the CA model; section 6 deals with implementation of GA to model urban growth; section 7 discusses the results of modeling the urbanisation process and its relation to public policy followed by concluding remarks in section 8.

2. Study Area

Bangalore city is the principal administrative, cultural, commercial, industrial, and knowledge capital of the state of Karnataka. The administrative jurisdiction was widened in 2006 by merging the existing area of Bangalore city spatial limits with 8 neighbouring Urban Local Bodies (ULBs) and 111 Villages of Bangalore Urban District to form Greater Bangalore. Bangalore has spatially grown more than ten times since 1949 from 69 square kilometers to 741 square kilometers in 2006. Now, Bangalore (figure 1) is the fifth largest metropolis in India currently with a population of about 7 million (Ramachandra and Kumar, 2008).

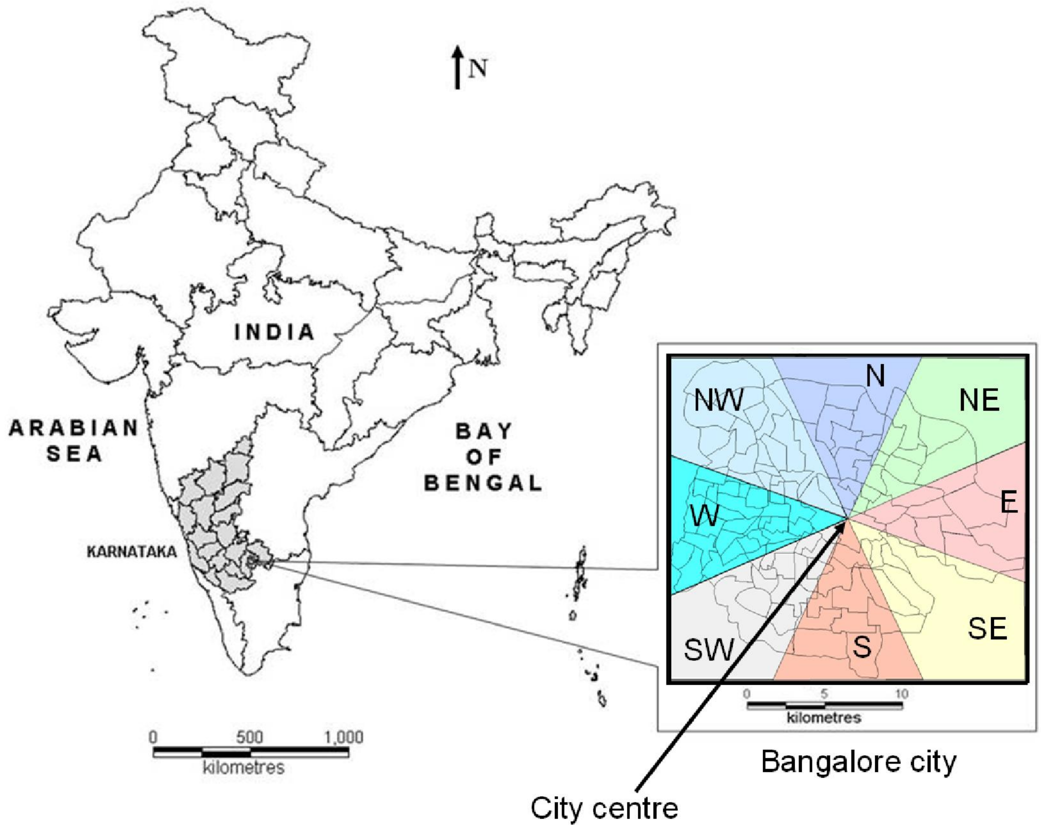

Figure 1: Study Area: Bangalore city, Greater Bangalore.

Bangalore city is composed of 100 wards. For our analysis, the city was divided into 8 zones [North (N), Northeast (NE), East (E), Southeast (SE), South (S), Southwest (SW), West (W), and Northwest (NW)] with their origin from the 'city centre' as shown in figure 1.

3. Data Preparation

This section describes the input data processing scheme. The two types of input data are:

(i) classified images of 1973, 1992 and 2006.

(ii) population density maps for the year 1973 and 1992.

Landsat Multispectral Scanner (MSS) of 1973 (in Blue (B), Green (G), Red (R) and Near Infrared (IR) bands of 79 m spatial resolution), Landsat Thematic Mapper (TM) of 1992 (B, G, R Near IR, Mid IR-1 and Mid IR-2 bands of 30 m spatial resolution), and IRS Linear Imaging Self

Scanner (LISS) - III of 2006 (in G, R and NIR bands of 23.5 m spatial resolution) were used for the generation of land use maps. The data are stored in 8-bit format, i.e. each pixel can take any value from 0 to 255 (2^8 = 256 values). The values of these pixels in the image are called digital numbers which represents the reflectance represented by that pixel corresponding to the same geographical location on the ground. The 1973 image was of size 429 rows x 445 columns, size of 1992 image was 1130 x 1170 and the size of 2006 image was 1445 x 1496. The differences in the size of the images are due to variations in the spatial resolution of the pixels (79 m, 30 m, and 23.5 m). These data were rectified and registered for systematic errors with the known ground control points that were identifiable in the image as well as Survey of India (SOI) topographical sheets of 1:50000 scale and projected to Polyconic system with Geographic Latitude-Longitude coordinate system and Evrest56 as the datum. All data were resampled to 23.5 m spatial resolution having 1445 rows x 1496 columns to fit each other spatially. Six classes of interest were identified from the false colour composite images: residential areas, commercial areas, roads, vegetation, water, and open land.

Supervised classification of the image was performed using the Maximum Likelihood classifier (MLC). MLC has become popular and widespread in remote sensing because of its robustness (Strahler, 1980; Conese and Maselli, 1992; Ediriwickrema and Khorram, 1997; Zheng et al., 2005). MLC assumes that each class in each band can be described by a normal distribution (Bayarsaikhan et al., 2009). For each land use class (residential areas, commercial areas, roads, vegetation, water, and open land) training samples were collected representing approximately 10% of the study area. With these 10% known pixel labels from training data, the aim was to assign labels to all the remaining pixels in the image.

If the training data (collected from the ground cover using handheld GPS - global positioning system) pertaining to land use classes contain n samples and the samples in each land use class are i.i.d (independent and identically distributed) random variables and further if we assume that the spectral classes for an image is represented by ω_i, i=1,…, M, where M is the total number of classes, then probability density $p(\omega_i|\mathbf{x})$ gives the likelihood that the pixel $\mathbf{x}$ belongs to class ω_i where $\mathbf{x}$ is a column vector of the observed digital number (gray values) of the pixels. It describes the pixel as a point in multispectral space (d-dimensional space, where d is the number of remote sensing spectral bands). The maximum likelihood (ML) parameters are estimated from representative i.i.d samples. Classification is performed according to

$$\mathbf{x} \in \omega_i \quad if \;\; p(\omega_i|\mathbf{x}) \; > \; p(\omega_j|\mathbf{x}) \text{ for all } j \neq i. \tag{1}$$

i.e., the pixel x belongs to class ω_i if $p(\omega_i|\mathbf{x})$ is the largest. The ML decision rule is based on a normalized (Gaussian) estimate of the probability density function of each class. The discriminant function for MLC is expressed as

$$\mathrm{g}_{\mathrm{li}}(\mathbf{x}) = p(\mathbf{x}|\omega_i)\, p(\omega_i) \tag{2}$$

where $\mathrm{g}_{\mathrm{li}}(\mathbf{x})$ stands for the discriminant function for ω_i, $p(\omega_i)$ is the prior probability of ω_i, $p(\mathbf{x}|\omega_i)$ is the p.d.f. for pixel vector $\mathbf{x}$ conditioned on ω_i (Zheng et al., 2005). Pixel vector $\mathbf{x}$ is assigned to the class for which $\mathrm{g}_{\mathrm{li}}(\mathbf{x})$ is greatest. In an operational context, the logarithm form of (2) is used, and after the constants are eliminated, the discriminant function for ω_i is stated as

$$\mathrm{G}_{\mathrm{li}}(\mathbf{x}) = (\mathbf{x} - M_i)^T \textstyle\sum_i^{-1} (\mathbf{x} - M_i) + \ln |\textstyle\sum_i| - 2 \ln P(\omega_i) \tag{3}$$

where $\sum_i$ is the variance-covariance matrix of ω_i, $\mathrm{M_i}$ is the mean vector of ω_i. A pixel is assigned to the class with the lowest $\mathrm{G}_{\mathrm{li}}(\mathbf{x})$ (Zheng et al., 2005; John and Xiuping, 1999, Duda, Hart and Stork, 2001).

Residential, commercial and roads were grouped into a single class – ‘urban’. Final classified images had four land use classes – builtup, vegetation, water and open land (others). The classified images of 1973, 1992 and 2006 had overall accuracies of 72%, 75%, and 73%. Classification was done using the open source programs (i.gensig, i.class and i.maxlik) of Geographic Resources Analysis Support System (http://wgbis.ces.iisc.ernet.in/grass) as displayed in figure 2. The classified images were also verified with field visits and Google Earth image. The class statistics is given in table 1.

Table 1: Greater Bangalore land use statistics

Class → Year ↓		Urban	Vegetation	Water Bodies	Open land
1973	**Ha**	5448	46639	2324	13903
	%	**7.97**	**68.27**	**3.40**	**20.35**
1992	**Ha**	18650	31579	1790	16303
	%	**27.30**	**46.22**	**2.60**	**23.86**
2006	**Ha**	29535	19696	1073	18017
	%	**43.23**	**28.83**	**1.57**	**26.37**

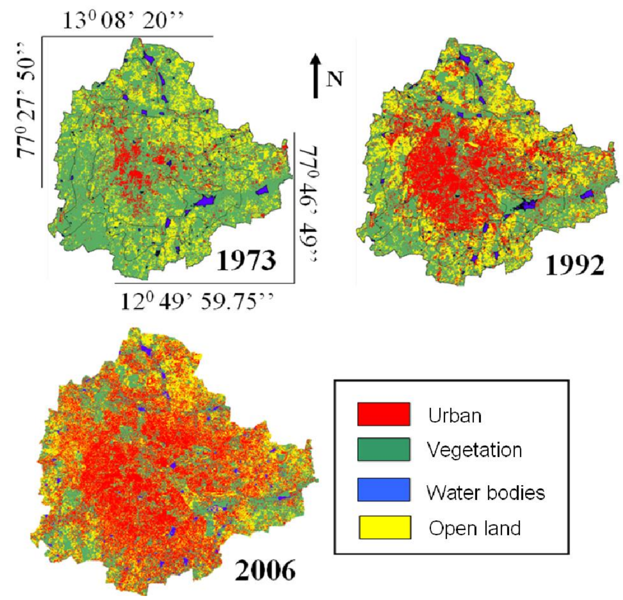

Figure 2: Greater Bangalore in 1973, 1992 and 2006.

Population density is used as the second input for the CA model algorithm. Population census maps for year 1971, 1991 and 2001 over Bangalore city were prepared from the census data. The population densities were computed for all 100 wards by dividing their populations by the ward areas. Figure 3 shows the ward map (left) in each direction and the density for each ward census (right) in 1971, 1991 and 2001. To model the population, the centroid (Xc, Yc) for each ward is calculated.

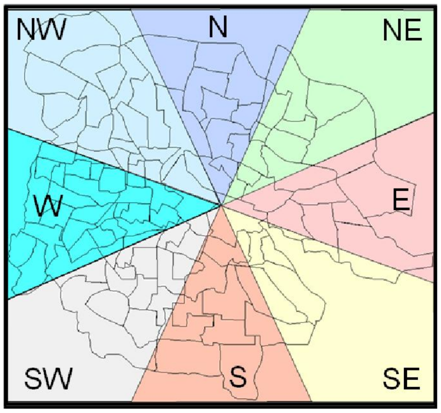

Ward No.	Ward	Distance	Density 1973	Density1991	Density2001
1	Vasanthnagar	1.32	400	2320	11981
2	Shivajinagar	2.11	777	3641	16252
3	Jayamahal	3.12	798	4292	18917
4	Koromangla	4.43	847	3316	23011
5	Austin Town	5.96	1925	4946	33429
6	Hebbal	6.49	273	3916	16068
7	Richmond Town	4.19	2901	9544	29139
8	Ganganagar	4.45	101	2622	23658
9	Sanjayanagar	6.24	61	3473	29221
10	J P Nagar	7.46	704	4704	19792

Figure 3: Ward map in each direction and their population densities. Distances are expressed in kilometers and population densities are expressed in persons/sq. km.

The Euclidean distance from each ward centroid to the city center (see figure 1) was computed. This process was repeated for all wards so that a table of population densities versus distance is prepared. Population densities for wards within specified distance from city center were averaged to reduce the variability in data. For example, an average population density for all wards within 0-1 km was calculated, then another average density is calculated for wards within 1-2, 2-3, 3-4 km and so forth. Curves were fitted representing population density as a function of distance from the city centre as shown in figure 4.

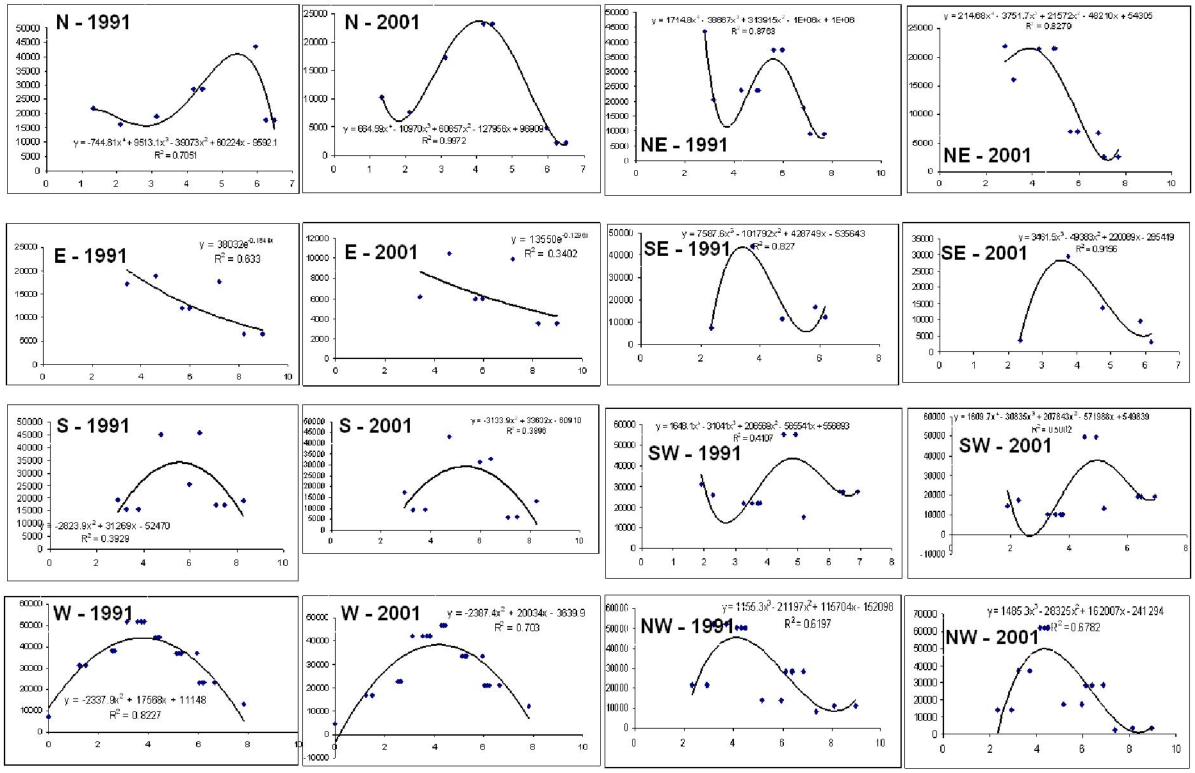

Figure 4: Direction wise population density for the year 1991 and 2001.

The unknown model parameters were calculated for the year 1991 and 2001. These models were used to calculate the population density for each pixel in the imagery based on its distance from the city centre for the year 1991 and 2001. The changes in model parameters over the 10 years (from 1991 to 2001) were used to calculate the yearly rate of change in model parameters. The updated parameters that changed year by year were used to calculate the population density grids for the year 1973 and 1992 matching the same size of the input imagery (remote sensing classified maps - 1445 rows x 1496 columns). These grids were used as the second CA data input for the purpose of running the model over historical growth period.

4. Cellular automata (CA) growth modeling

This section discusses in detail the design of the CA urban growth modeling. The design phases include: transition rule definition, calibration method and evaluation strategy for the model. Calibration modules for accurate modeling over the historical satellite imagery to adapt the urban pattern.

4.1 CA algorithm design

The design of the CA algorithm consists of defining the transition rules that control the urban growth, calibrating these rules, and evaluating the results for prediction purpose as shown in figure 5. Transition rules definition is the most important phase in CA model design since they translate the effect of input data on the urban process simulation. The CA algorithm design starts with defining the transition rules that drive the urban growth over time. They are designed as a function of land use effect on urban process, growth constraints and population density. The transition rules are defined over the 3 x 3 neighbourhood of a pixel to minimize the number of input variables to the model. The rules identify the neighbourhood needed for the tested cell to urbanise.

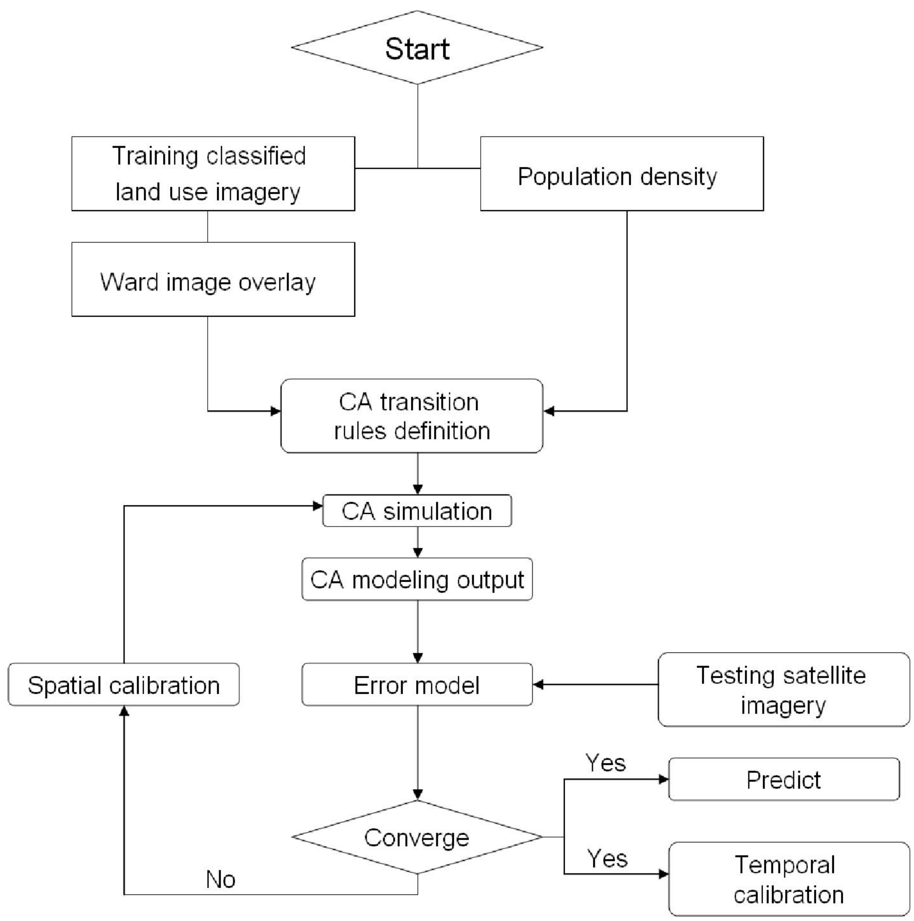

Figure 5: Flowchart of CA algorithm design.

The growth constraints should reflect the conservation strategy adopted in the study area for certain land uses. For example, conservation of certain species of natural resources can be taken into consideration through rules definition stage. Water resources protection through discouraging urban growth nearby these sites to preserve them over time is another example of constrained rules design. The future state of a pixel (Equation 4) at time ($t+1$) from starting time (t) depends on three factors:

- Current state of the pixel
- Current states of the neighbourhood pixels
- Transition rules that drive the urban growth over time

$$S^{t+1}(\alpha) = f(S^{t}(\alpha), S^{t}(\tau), transition\_rules) \quad \ldots.. \quad \text{(Equation 4)}$$

where

$S^{t+1}(\alpha)$ = test pixel future state at time epoch t+1
$S^{t}(\alpha)$ = test pixel current state at time epoch t
$S^{t}(\tau)$ = neighbourhood pixels states' set.

4.2 CA Model calibration

Calibration aims to define the best set of CA rules based on which the model runs to match as close as possible to the simulated results with the ground truth images. To achieve this purpose, two calibration schemes are introduced in this algorithm: spatial and temporal calibrations. In spatial calibration module, the CA transition rules at a given time t are modified spatially over the 2D grid space. This is done through tuning the values of each rule set on a directional basis to match the urban dynamics for each township with its site specific features. This allows the model to take the variability in the spatial urban growth pattern into account for realistic modeling. If the CA rules in a direction result in higher growth levels (overestimated), they are modified to reduce the urban growth in that direction. For the underestimation case, the rule values of the direction under consideration are tuned to increase the amount of urban growth to match the real one. So, the spatial calibration aims to find the best set of rule values that fit a given direction according to its geographical location.

The oldest historical classified Landsat MSS image (of 1973) subset for Bangalore city (figure 6) from the Greater Bangalore image (figure 2) is used as input to the CA model over which the transition rules are applied to model the urban growth starting from this time epoch. Dividing the study area on a direction and further on a ward basis will take into consideration the effect of site specific features in each direction on the urban growth. The same CA transition rules are defined for each direction, however, with different rule values. CA transition rules (ϕ) of the developed model were physically built over the input imagery and the rules used a 3 x 3 neighbourhood - $A_{i,j}^{t}$ in equation 5 to identify the test pixel future state, $a_{i,j}^{t+1}$ in equation 6.

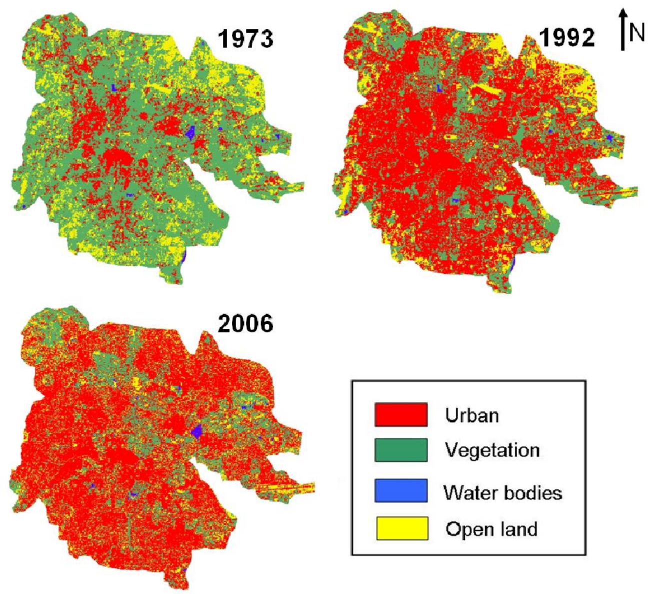

Figure 5: Bangalore city in 1973, 1992 and 2006 used in the CA model for simulation (subset from Greater Bangalore classified image).

$$A_{i,j}^{t} = \begin{bmatrix} a_{i-1,j-1}^{(t)} & a_{i-1,j}^{(t)} & a_{i-1,j+1}^{(t)} \\ a_{i,j-1}^{(t)} & a_{i,j}^{(t)} & a_{i,j+1}^{(t)} \\ a_{i+1,j-1}^{(t)} & a_{i+1,j}^{(t)} & a_{i+1,j+1}^{(t)} \end{bmatrix}_{3x3neighbourhood} \qquad \ldots.. \qquad \text{(Equation 5)}$$

$$a_{i,j}^{t+1} = \phi(A_{i,j}^{t}) \qquad \ldots.. \qquad \text{(Equation 6)}$$

Transition rules (ϕ) were designed to identify the required neighborhood urban level for a test pixel to urbanise. The following is a summary of such rules:

1. IF test pixel is water, road OR urban (residential or commercial) THEN no change.
2. IF test pixel is non-urban (vegetation OR open land) THEN it becomes urban if its:
   - Population density is equal or greater than threshold (*Pi*) AND neighbouring residential pixel count is equal or greater than threshold (*Ri*)

where $(R,C)_i$ are integer numbers ranging from 0 to 8 (*3* x *3* neighborhood) and *Pi* is a real number ranging from 0 to 1 (0.1 increment; population density values were normalized from 0 to 1 for each direction in order to have effective CA rules calibration). The calibration (i.e., identifying best $(R,P)_i$ parameter values) of such rules was performed spatially on a ward level, *Tw* to fit the local urban dynamic features and over time to consider the temporal urban changes in each direction, T_t in (7).

$$Ø_{calibrated} = f(T_w, T_t, \phi) \qquad \text{..... (Equation 7)}$$

ϕ in the calibration formula represents the criteria selected to find the best rule set for certain ward spatial location T_w at given time epoch T_t. This criterion in our model represents the total modeling errors/mismatch between modeled output and reality that need to be minimised or best match. ϕ in (8) was defined as a function of fitness *F* in (9) and total errors ΔE in (10) valuation measures. Fitness and total errors measure the compatibility in terms of urban count and pattern within each township with respect to reality, respectively (Al-Kheder, et al., 2007).

$$\phi = Abs(F - 100\%) + \Delta E \qquad \text{..... (Equation 8)}$$

$$F = \frac{Modele\_urban\_count}{Ground\_truth\_urban\_count} \times 100\% \qquad \text{..... (Equation 9)}$$

$$\Delta E = \frac{Total\_error\_count}{Total\_count} \times 100\% \qquad \text{..... (Equation 10)}$$

Once the CA transition rules were identified and initialized for each direction, the model runs from 1973 till 1992. The 1992 image represents the first ground truth being used for calibration. For each ward, the modeling accuracy is calculated as a ratio between the simulated and real urban growth data. Over/underestimation concept is introduced to represent how comparable is the simulated result to the real one. This indicates how transition rules defined on a directional basis succeed in modeling the real amount of urban growth given the predefined conditions. Calibration in this work is meant to find the best set of rule values specific to each direction for realistic urban growth modeling.

5. Results

Simulation and prediction urban modeling results, as shown in table 2 and figure 6 shows a less close match to the reality from 1973 to 1992 in terms of urban count, however, the pattern matches in various directions to some extent.

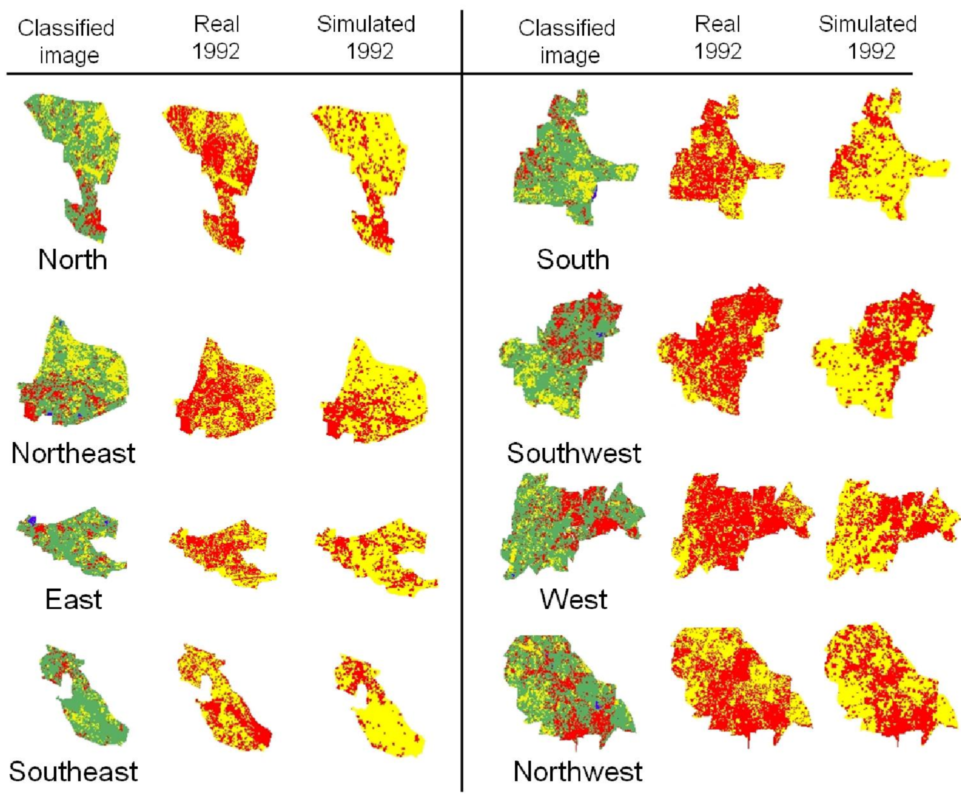

Figure 6: Classified image of 1973, real image and simulated image of 1992. Red colour indicates urban areas, yellow represents other classes (vegetation, water or open land) in real and simulated images.

Table 2: Numerical evaluation results

Direction	**1973 Simulation / 1992 Prediction**			**1992 Simulation / 2006 Prediction**		
	Fitness %	***Total Error, ΔE%***	ϕ	***Fitness %***	***Total Error, ΔE%***	ϕ
North	52.58	32.39	79.82	101.71	30.82	32.53
Northeast	66.43	30.48	64.05	101.66	35.44	37.10
East	65.51	39.82	74.31	99.87	40.68	40.81
Southeast	42.28	29.72	87.44	99.89	36.86	36.97
South	46.39	33.33	86.93	105.36	29.18	34.54
Southwest	58.55	16.71	58.16	100.58	23.24	23.81
West	61.35	17.22	55.87	100.80	21.15	21.96
Northwest	86.13	33.08	46.95	102.90	36.08	38.98
Average	59.90	29.09	69.19	101.60	31.68	33.33

The reason for the mismatch of the urban pixels is that the growth from 1973 to 1992 has happened haphazardly which has not been reflected and captured by the change in population density of various wards in different directions. In contrast the simulated images of 2006 (figure 7) are more close to the real classified image in terms of the urban count.

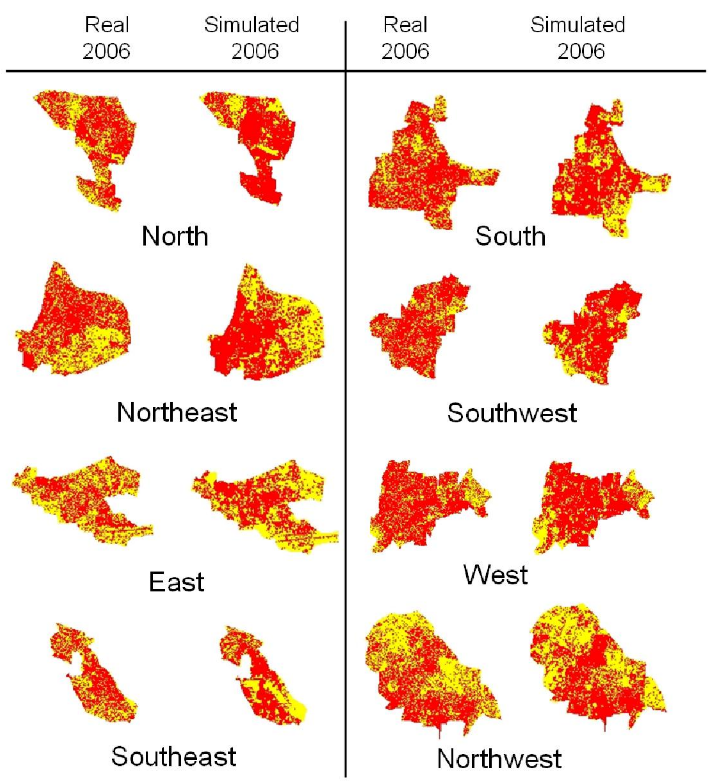

Figure 7: Real image and simulated image of 2006. Red colour indicates urban areas, yellow represents other classes (vegetation, water or open land).

6. Implementation of Genetic Algorithm (GA)

This section introduces briefly the on going study on using genetics algorithm (GA) to automate the spatial and temporal rule calibration. GA as a heuristic optimisation technique can work over the search space to find the most suitable solution. GA improves the efficiency of rule calibration to select the best set of rule values for accurate modeling. GA was first introduced by Holland (1975) as computer programs to mimic the evolutionary process in nature. GA manipulates a set of feasible solutions to find an optimal solution and is able to find the global optimum solution (S. Alkheder and J. Shan, 2006). The following steps describe the design of the proposed GA-based transition rule calibration.

Step 1: Initial GA population generation: In this step, 30 set of rule values were randomly generated as an initial population for each direction over which GA module would work. Each rule value set was coded as a binary string and a string was designed as a combination of the rule values. Two rules were identified to be optimised using GA.

> **Rule 1:** The number of neighbourhood urbanised (residential plus commercial) pixels, in the possible range of [0-8] integer values or in corresponding binary coding [0000 to 1000].
>
> **Rule 2:** The population density threshold, continuous values represent the cut-off population density at a pixel. This rule was scaled by multiplying its value by 10 in the range of [0-10] possible values or in binary coding [0000 to 1010].

Step 2: Fitness function identification: Fitness function evaluates the performance of each string. The prediction accuracy was used as the fitness function.

Step 3: GA selection operation: Rank selection procedure was used here. All the strings were ordered based on their fitness values in descending order and the string with highest fitness value was given rank 30 then the second one 29 till lowest fitness value with rank 1. Rank was divided by the summation of all the ranks and the probability of selection for each string in next generation was identified.

Step 4: GA crossover and mutation parameters design: The crossover probability was selected to be 80%, 24 strings were selected for crossover, while the other 6 (the best 6 in terms of fitness values) were copied directly to the new generation (this process is known in GA as Elitism). Elitism can rapidly increase the performance of GA, because it prevents a loss of the best solution. A mutation rate of 1% was used. Once the crossover and mutation was done, the new generation of 30 strings was produced and the loop continued. This continued until the convergence criterion was met. The final output was the optimized CA rule values that model the temporal urban growth. The model is run over the western region of the city to project the growth in 2006 using 1992 data. The final result (figure 8) indicates good match (94 %) with the real 2006 classified image.

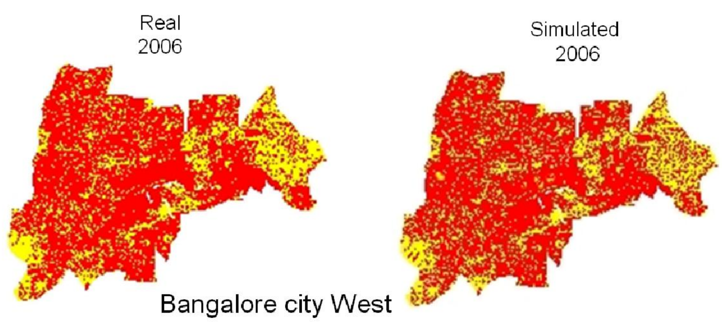

Figure 8: GA-CA calibrated results for the year 2006.

7. Discussion on results of modeling the urbanisation and its relation to public policy

Prediction accuracy for each direction is used as a basis for rule calibration. Over/under estimation principle was implemented. If a set of rules for a particular direction produced underestimated results, this mean the growth rate is small and hence the rules are modified to increase the urban growth. For overestimation, the rules were modified to reduce the urban growth amount. The transition rules for a direction were repeatedly calibrated till the convergence criterion is met. The classified image provides the reference for calibration process. In table 2, the *Fitness %, Total Error (ΔE %)* and ϕ values for the year 1992 indicates a poor match of the simulated image with the real image (classified image), which is an indication of underestimation of urban pixels in various directions. However, the results for the 2006 simulated image (table 2), indicates very good spatial prediction accuracy. The spatial variability between the various directions as compared to the real image is small. This indicates the effect of spatial calibration in matching each direction with its realistic urban growth pattern through calibrating its rules. It also helped in capturing finer details in the modeling process while calibrating the model over smaller spatial units to reduce modeling uncertainty. Visually, calibration on a directional basis succeeds in preserving the urban pattern over space and over time. Rule values' results at the end of the calibration process indicate some similarity between growth in various directions such as the east, west and the northwest. These wards have almost the same growth rate and pattern because of similar infrastructure, facilities, and more open area for outer growth and urban sprawl. Most of these similar wards have ring roads or highways passing through them that allow linear urban growth happening along.

The average fitness value for the 1992 image was ~ 60% and the total error was 29.09 with an approximate match of 71%. It is to be noted that for a highly accurate prediction, the total modeled urban count and ground truth urban count will be equal and therefore the fitness value (F) will be 1 or 100%. The total errors ΔE is the error of omission and commission. More the value of ΔE, more is the percentage of error count. There seems some mismatch between the urban pixels in 1992 that is without any visible pattern and therefore could not be assessed and captured by the change in population density contours and curve fits in various wards and different directions. Simulation and prediction urban modeling results, as shown in table 2 for the year 2006, show that the fitness results for prediction was close in terms of urban count (values close to 100%) between the modeled and real data with average fitness of 101.60 (little overestimate) and the average total error of 31.68% was achieved. This indicates an approximate match level of 69% on a pixel by pixel basis between modeling and reality. Therefore, higher the value of ϕ in equation 8, higher is the modeling error. For the 2006 simulated image, the average ϕ is 33.33 showing a more realistic result as compared to the actual urban growth pattern. This is a high accuracy level compared to the results shown in literature for the urban land spatial fit area that was only 28.15 to 44.6% (Yang and Lo, 2003). The close urban pattern match is also clear in figure 6 where the simulated images have urban distribution similar to those shown in their corresponding real images.

The simulation results of urban growth should be accurate and should represent the actual local site specific patterns close to reality since urbanisation process is directly linked to society, infrastructure, level of services, etc. At this point of time, it would be appropriate to link *people-and-pixels* in remotely sensed images. One rationale for doing so is that, it might result in better social science research in several ways – such as measuring the context of social phenomena and their effects while providing additional measures, making connections across levels of analysis, providing time-series data on socially relevant phenomena. On the other hand, social science has also to play a major role for remote sensing. Social science makes several kinds of scientific contributions to remote sensing such as validation and interpretation of remote observations, data confidentially and public use, etc. Together remote sensing mapping technology and social science can improve understanding of human-environment interactions to a great extent. They help in interpreting, modeling, predicting the dynamics of natural resources, and in understanding the human consequences of climate flux, etc.

The change in land use such as agricultural fields, buildings, roads are often considered human artifacts and gets less importance and are therefore less interesting than the abstract variables that explain their appearance and transformations. Changing land use are regarded as manifestations of more important variables, such as government policies, land-tenure rules, distribution of wealth and power, market mechanisms, and social customs, none of which are directly reflected in the bands of the electromagnetic spectrum. The social utility argument posits that the interpretation of classified images obtained from remote sensing imageries becomes even more valuable to the extent that social scientist find useful, and that efforts should be made to identify and overcome the existing barriers to making this happen. From the perspective of social science, one important reason for using remotely sensed data is to gather information on the context that shapes social phenomena. The role of context has been central to the theories and empirical work of numerous statisticians, sociologists, economists, and anthropologists. In this context, remote sensing technology offers an additional source of contextual data for multilevel analyses.

Another consideration involves the growing interdisciplinary community ranging from sustainable development, pollution prevention, global environmental change, to related issues of human-environment interaction who need to compare data on social and environmental phenomena at the same spatial and temporal scales (Liverman et al., 1998). Therefore, the consideration of spatial and temporal resolutions is very important.

Another critical issue in linking people with pixels and image is the decision on where to gereference individuals or other social units. The approach adopted in this work aggregates social data to larger geographical units; assigning individuals to larger areas in which their environmental effects are more likely to be confined. It is necessary at this point of time, to socialise the pixel and pixelise the social in land use and land cover change. Mining the pixel involves seeking social meaning in imaginary – information and indicators relevant to such concerns as economic well-being or criticality, perhaps signaling the underlying processes that give rise to land use and land cover change. This meaning is often hidden deep within the analysis of the imagery and this depth may impede such investigation. A paucity of spatially explicit data has constrained spatial modeling of human behavior and social structures, especially beyond the field of geography and has fostered modeling approaches that abstract the essential spatial nature of the problem. As a result, either aggregate relationships are specified, or the spatial components in a model are reduced to unidimensional variables, such as the distance between economic activities in location model, the wage differential in a migration model, or the cost of access in a transportation model. The increased availability of spatially explicit data, both remotely sensed and other data, and GIS (Geographic Information System) has begun to change the situation. Advances are being made to link on-the-ground human actions and consequences to imagery (pixels) through models, or modeling to the pixel, as in modeling the determinants of the decision of individual land managers on the basis of utility maximisation, satisficing, or other theories of human behavior. The use of pixels may extend to explain the dynamics of many indicators such as energy demand and conservation, environmental area assessment, disaster energy response, forecasting urban expansion that can be visualized as concentric rings, sectors or multiple nuclei.

The future interaction between societal studies and remote sensing depends on what kind of features can be detected and how often data can be obtained. Remote sensing technology may be used not only for monitoring change, but also for conducting surveillance. For example to count houses, to count the number of stories in each house, and detect changes in building structure. This may provide ability to check on building regulations and thus develop some new surrogates for social economic conditions. The key question is whether this type of information can be used to create more efficient urban environments and provide a more equitable distribution of resources and services?

8. Conclusion

This work explores the potential of implementing the cellular automata to model the historical urban growth over Bangalore city. The main goal is to design the model as a function of local neighbourhood structure to minimise the input data to the model. Satellite imagery represents the medium over which the model works. One special issue the model takes into account is the calibration process. Two modules were used namely, spatial and temporal calibration. Spatial calibration fits the model on a directional basis to its site specific feature while the temporal calibration adapts it to the urban growth dynamic change over time. This is a noticeable effect on producing a good spatial match between the real and simulated image data. On the other hand, GA is introduced to enhance the CA calibration process. GA makes the calibration process more efficient through manipulating a set of feasible solutions in the search space to find an optimal solution. This will reduce the search space for the optimal rules' values on a directional basis. The above techniques are robust in predicting urban growth and visualizing them through pixels in images. Relating pixels in remote sensing data and people in society is important for studies on sustainable development, pollution prevention, global environmental change, and issues of human-environment interaction at different spatial and temporal scales.

9. References

Alkheder, S, Shan, J., 2006, 'Change detection - cellular automata method for urban growth modeling', *International Society of Photogrammetry and Remote Sensing Mid-term Symposium*, WG VII/5, Netherlands, May 2006.

AlKheder, S., Wang, J., and Shan, J., 2007**, '**Cellular automata urban growth model calibration with genetic algorithms', *Urban Remote Sensing Joint Event*.

Batty, M., and Xie, Y., 1994, 'From cells to cities', *Environment and Planning*, B21, pp. 531-548.

Bayarsaikhan, U., Boldgiv, B., Kim, K-R., Park, K-A., Lee, D., 2009, Change detection and classification of land cover at Hustai National Park in Mongolia. International Journal of Applied Earth Observation and Geoinformation, 11, 273-280.

Conese, C., Maselli, F., 1992, Use of error matrices to improve area estimates with maximum likelihood classification procedures. Remote Sensing of Environment, 40, 113-124.

Clarke, K. C., Hoppen, S., and Gaydos, L., 1997, 'A selfmodifying cellular automaton model of historical urbanization in the San Francisco Bay area', *Environment and planning*, 24, pp. 247-261.

Clarke, K. C., and Gaydos, L. J., 1998, 'Loose-coupling a cellular automaton model and GIS: long-term urban growth prediction for San Francisco and Washington/Baltimore', *International Journal of Geographical Information Sciences*, 12, pp. 699-714.

Duda, R. O., Hart, P. E., and Stork, D, G., 2000, *Pattern classification*, New York, A Wiley-Interscience Publication, Second Edition, ISBN 9814-12-602-0.

Ediriwickrema, L., Khorram, S., 1997, Hierarchical maximum-likelihood classification for improved accuracies. Geoscience and Remote Sensing, IEEE Transactions, 35, 810-816.

Hagerstrand, T., 1967, ‘Innovation Diffusion as a Spatial Process’ University of Chicago Press, Chicago, IL.

Holland, J. H., 1975, ‘Adaptation in Natural and Artificial Systems’, Univ. of Michigan Press, Ann Arbor, MI.

John, A. R., Xiuping, J., 1999. Remote Sensing Digital image Analysis: An Introduction. Springer-Verlag Inc., New York.

Li, X., and Yeh, A. G. O., 2003, ‘Error propagation and model uncertainties of cellular automata in urban simulation with GIS’, *In:7th International Conference on GeoComputation*, 8- 10, September 2003, University of Southampton, Southampton, UK (GeoComputation CD-ROM).

Liverman, D., Moran, E. F., Rindfuss, R. R., and Stern, P. C., 1998, *People and pixels - Linking Remote Sensing and Social Science*, Washington, D. C., National Academy Press.

Ramachandra, T.V., and Kumar, U., 2008, ‘Wetlands of Greater Bangalore, India: Automatic Delineation through Pattern Classifiers’, *Electronic Green Journal*, Vol. 26**,** Spring 2008 ISSN: 1076-7975.

Strahler, A. H., 1980. The use of prior probabilities in maximum likelihood classification of remotely sensed data. Remote Sensing of Environment, 10, 135-163.

Tobler, W., 1979, ‘Cellular geography, in Philosophy’, In: Geography Eds S Gale, G Olsson (D Reidel, Dordrecht), pp. 379-386.

von Neumann, J., 1966, ‘Theory of Self-Reproducing Automata’, University of Illinois Press, Illinois. Edited and completed by A. W. Burks.

White, R. and Engelen, G. 1992. "Cellular Dynamics and GIS: Modeling Spatial Complexity", position paper presented at the NCGIA Specialist Meeting on GIS and Spatial Analysis.

White, R. and Engelen, G. 1993. "Cellular Automata and Fractal Urban Form: A Cellular Modeling Approach to the Evolution of Urban Land Use Patterns", Environment and Planning A, 25, 1175-1199.

Wolfram, S., 1994, 'Cellular automata', *In: Cellular Automata and Complexity: Collected Papers*, Addison Wesley, Steven Wolfram, Reading, MA.

World Urbanization Prospects, 2005, Revision, Population Division, Department of Economic and Social Affaris, UN.

Yang, X, and Lo, C. P., 2003, 'Modelling urban growth and landscape changes in the Atlanta metropolitan area', *International Journal of Geographical Information Science*, Vol. 17, pp. 463–488.

Zheng, M., Cai, Q., Wang, Z., 2005. In: Effect of prior probabilities on maximum likelihood classifier. Geoscience and Remote Sensing Symposium, 2005, IGARS'05, Proceedings 2005 IEEE International, 6, pp. 3753-3756.

Uttam Kumar is a PhD student at the Department of Management Studies and Centre for Sustainable Technologies, Indian Institute of Science, Bangalore. His areas of research are developing algorithms for multi-satellite sensor spatial temporal data analysis. His research interests are Pattern recognition, Remote sensing, Data mining and Image processing.

Chiranjit Mukhopadhyay earned a Ph.D. in Statistics from University of Missouri, Columbia in 1992, after obtaining M-Stat and B-Stat from Indian Statistical Institute, Kolkata. Currently he is Associate Professor of Statistics in the Department of Management Studies, Indian Institute of Science, Bangalore. He has served in the faculty of several Universities around the globe like The Ohio State University, Case Western Reserve University, Bilkent University etc. His current research interests include Bayesian Statistics, Reliability Theory, Statistical Quality Control, Empirical Finance and Financial Econometrics.

Ramachandra T. V. obtained his Ph.D. from Indian Institute of Science (IISc), Bangalore. Currently he is a faculty at the Centre for Ecological Sciences (CES), Centre for Sustainable Technologies (CST) and Centre for Infrstructure, Sustainable Transport and Urban Planning (C*i*STUP) at IISc, Bangalore. His area of research includes remote sensing, digital image processing, urban sprawl: pattern recognition, modelling, energy systems, renewable systems, energy planning, energy conservation, environmental engineering education, etc. He has published 108 research papers in national and international journals, and has more than 75 papers in conferences. He has written 14 books on related topics. He is member of many national and internationally recognized professional bodies and is also the Convenor, Energy Information System (ENVIS) at IISc. He is a Member of Karnataka State level Environment Expert Appraisal Committee (2007-2010), appointed by the Ministry of Environment and Forests, Government of India and a member of Western Ghats task force appointed by the Government of Karnataka. He is a recipient of 2007 Satish Dhawan Young Engineer Award, 2007 of Karnataka State Government.